molbank

MDPI

Short Note

Benzyl-*N*-[4-(2-hydroxyethyl)-1,3-thiazol-2-yl]carbamate

Lucrezia Spinelli, Matteo Mori and Laura Fumagalli *

Department of Pharmaceutical Sciences, University of Milan, 20133 Milan, Italy; lucrezia.spinelli@studenti.unimi.it (L.S.); matteo.mori@unimi.it (M.M.)
* Correspondence: laura.fumagalli@unimi.it

Abstract

Heterocycles—cyclic compounds containing at least one non-carbon heteroatom (e.g., N, O, S)—are fundamental in medicinal chemistry due to their influence on a drug's physicochemical and biological properties. They improve solubility, bioavailability, and facilitate molecular recognition through their electronic and hydrogen-bonding features. These properties make them indispensable in drug design. This study focuses on the synthesis of a key heterocyclic intermediate: benzyl-*N*-[4-(2-hydroxyethyl)-1,3-thiazol-2-yl]carbamate. This molecule incorporates a thiazole ring, known for its rigidity and electronic properties, that enhances target interactions. The 2-position bears a Cbz-protected amine, enabling orthogonal deprotection, while the 4-position features a hydroxyethyl side chain, providing a handle for further chemical modifications via nucleophilic substitution. Herein, we report the successful synthesis of this intermediate along with its full ^{1}H and ^{13}C NMR spectra, melting point, and crystal structure, confirming its identity and purity.

Keywords: 2-amino-thiazol-4-yl-ethyl; thiazole; NMR-spectroscopy; X-ray crystallography

1. Introduction

Heterocyclic compounds, so defined since they contain at least one heteroatom—such as nitrogen, oxygen, sulfur—in a cyclic structure, are derived from natural products or obtained by chemical synthesis in the laboratory [1–3]. The non-carbon atoms profoundly influence the physical, chemical, and biological properties of these compounds, which are particularly important when they are used as drugs. Heterocycles typically give the molecule better solubility and salt-forming propensity, which enhances the pharmacokinetic properties, including oral absorption and bioavailability [4]. Thus, by incorporating heterocycles, medicinal chemists can tune lipophilicity, polarity, solubility, and metabolic stability. Finally, heterocycles play a crucial role in target binding and molecular recognition by exploiting their unique electronic structures and hydrogen-bonding capabilities. For these reasons, synthetically accessible and pharmacologically relevant heterocycle intermediates are extremely useful in medicinal chemistry for designing and developing novel therapeutic agents. One such molecule is benzyl-*N*-[4-(2-hydroxyethyl)-1,3-thiazol-2-yl]carbamate (Figure 1), a highly versatile compound that combines multiple functional elements critical for drug synthesis. Structurally, this intermediate features a thiazole ring substituted at the 2-position by a benzyloxycarbonyl (Cbz)-protected amine and at the 4-position by an ethyl chain bearing an alcoholic function.

check for updates

Academic Editor: Stefano D'Errico

Received: 27 June 2025
Revised: 15 July 2025
Accepted: 16 July 2025
Published: 21 July 2025

Citation: Spinelli, L.; Mori, M.; Fumagalli, L. Benzyl-*N*-[4-(2-hydroxyethyl)-1,3-thiazol-2-yl]carbamate. *Molbank* **2025**, *2025*, M2040. https://doi.org/10.3390/M2040

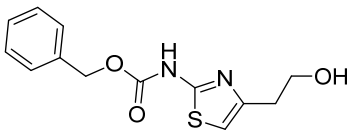

Figure 1. Benzyl-*N*-[4-(2-hydroxyethyl)-1,3-thiazol-2-yl]carbamate.

The thiazole moiety is a well-established, privileged structure in medicinal chemistry due to its rigid planarity, electronic properties, and hydrogen-bonding potential, all of which contribute to favorable interactions with biological targets. The Cbz-protected amine allows orthogonal deprotection and further derivatization, while the alcoholic function can be transformed to facilitate nucleophilic substitution, enabling the rapid construction of more complex, bioactive molecules. This combination makes the compound exceptionally valuable in combinatorial synthesis, fragment-based drug discovery, and late-stage functionalization—core strategies in the pharmaceutical industry, as demonstrated by the presence of the 2-amino-thiazol-4-yl-ethyl substructure in several classes of clinically important drugs (Figure 2) [5–9].

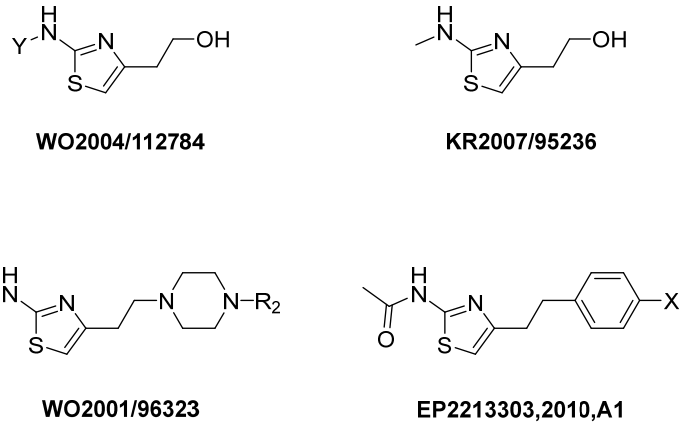

Figure 2. Clinically important drugs containing the 2-amino-thiazol-4-yl-ethyl moiety claimed in patents.

Herein, we report the synthesis of this key synthetic building block along with its ^{1}H and ^{13}C NMR spectra, melting point, and crystal structure.

2. Results and Discussion

To synthesize benzyl-(4-(2-hydroxyethyl)thiazol-2-yl)carbamate (Scheme 1), we slightly modified the procedure reported by Inoue et al. [10]. We began by dissolving methyl 2-(2-(((benzyloxy)carbonyl)amino)thiazol-4-yl)acetate in tetrahydrofuran (THF), followed by the portionwise addition of lithium borohydride ($LiBH_4$) at −10 °C. The reaction mixture was gently warmed to room temperature and stirred until the ester was completely reduced. The reduction was monitored by thin-layer chromatography (TLC) using cyclohexane/ethyl acetate 7:3 as the mobile phase (Rf **1** = 0.6, Rf **2** = 0.2, see Supplementary Materials).

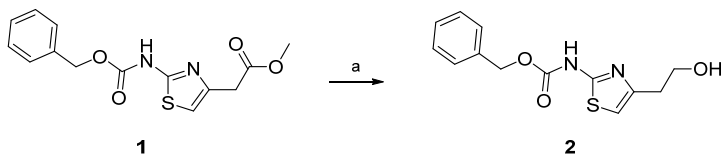

Scheme 1. Reagents and conditions for the synthesis of Benzyl-(4-(2-hydroxyethyl)thiazol-2-yl)carbamate: (a) $LiBH_4$, THF, RT.

The achievement of the title compound (**2**) was confirmed by ^{1}H and ^{13}C NMR.

Looking at ^{1}H NMR, the methylene protons attached to the thiazole ring resonate at 2.81 as a triplet of doublets (td, J = 6.7, 0.9 Hz, 2H), while the methylene adjacent to the oxygen appears at 3.80 ppm as a triplet (t, J = 6.7 Hz, 2H). The unique proton of the thiazole moiety resonates as a triplet at 6.69 ppm (t, J = 0.9 Hz, 1H). Additionally, the aromatic region of the spectrum presents a multiplet in the range 7.46–7.26 ppm, which corresponds to protons belonging to the benzyloxycarbonyl (Cbz) protection (m, 5H).

The ^{13}C spectrum shows all the expected carbons. The carbonyl carbon of the Cbz group appears at 173.79 ppm, while the signals corresponding to the thiazole ring are observed at 160.02, 148.75, and 107.78 ppm. Chemical shifts for the CH carbons of the phenyl ring appear at 128.17 ppm, 127.99 ppm, and 127.82 ppm, the quaternary carbon adjacent to the benzylic group at 135.92, and the benzylic CH_2 at 67.21 ppm, while the carbonyl carbon is observed at 154.00 ppm. The signal at 60.65 ppm corresponds to the aliphatic CH_2 attached to the hydroxyl group, while the central CH_2 appears at 34.02 ppm. Thus, both the spectra are consistent with the structure of compound **2**.

Additionally, compound **2** was analyzed by single-crystal X-ray diffraction to further confirm the success of the reduction and study the structural features of this class. The compound crystallized in the monoclinic system with the space group $P2_1/c$. The asymmetric unit, shown as an ellipsoid diagram in Figure 3, contains one molecule of compound **2**. The terminal C-OH of the flexible hydroxyethyl side chain is disordered over two positions, with a refined occupancy of 7:3; atoms corresponding to the minor component (30%) are labeled with the suffix A (Figure 3).

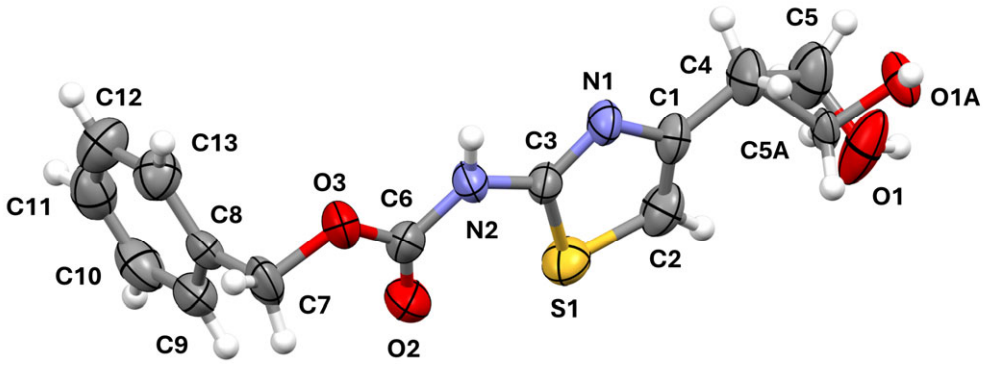

Figure 3. Thermal ellipsoid diagram of compound **2**, with the arbitrary atom-numbering scheme. Displacement ellipsoids are drawn at the 40% probability level.

The molecule features a planar core, composed of the thiazole and carbamate moieties. The phenyl ring of the Cbz group is inclined at 76.0° relative to the main plane, forming a torsional angle of −83.4 (6)° for C8-C7-O3-C6. The disordered hydroxyethyl chain adopts two distinct torsional angles: −74.0 (1)° for C1-C4-C5-O1 and −169.0 (1)° for C1-C4-C5A-O1A. The crystal packing is dominated by hydrogen bonding (Figure 4). The carbamate NH forms intermolecular hydrogen bonds with the thiazole nitrogen, resulting in centrosymmetric dimers extending along the c axis. This interaction appears to influence the geometry of the thiazole ring, reducing the C1–N1–N3 angle to 109.6 (5)°, which is statistically smaller than that observed in most thiazole-containing structures [11]. This effect has also been reported in other similar structures from the literature [12]. Additionally, the hydroxyl groups engage in hydrogen bonding with neighboring molecules, generating zipper-like chains that propagate along the b axis. This geometry implies a possible disorder of the hydroxyl hydrogen over two equivalent sites. However, the electron density is not sufficiently clear to model the atom with confidence, likely due to the modest resolution and local disorder. Interestingly, the A-labeled component exhibits less favorable hydrogen-

bonding geometry compared to the major conformer, which is consistent with its lower refined occupancy. The absence of a Cπ–H···O interaction in this minor conformer further contributes to its reduced stability. A full account of the hydrogen bonds is shown in Table 1. π-π stacking interactions also play a role in the stabilization of the packing (Figure 4). In detail, the phenyl rings of the Cbz moieties of adjacent molecules form an offset parallel stacking interaction with a centroid–centroid distance of 4.92 Å, as well as a T-shaped interaction with a centroid–centroid distance of 5.53 Å. Moreover, the thiazole cores also engage in offset parallel heteroaromatic stacking interactions, with a centroid–centroid distance of 4.92 Å. Finally, a geometry check of the molecule was performed using the *Mogul* routine [11], which compares molecular geometries to empirical distributions from the Cambridge Structural Database, providing valuable insight into structural features, as demonstrated in our previous study [13]. The analysis showed that most bond lengths and angles fall within typical ranges, except for the previously mentioned C1–N1–N3 angle and the disordered region, which is expected due to the flexibility of the side chain.

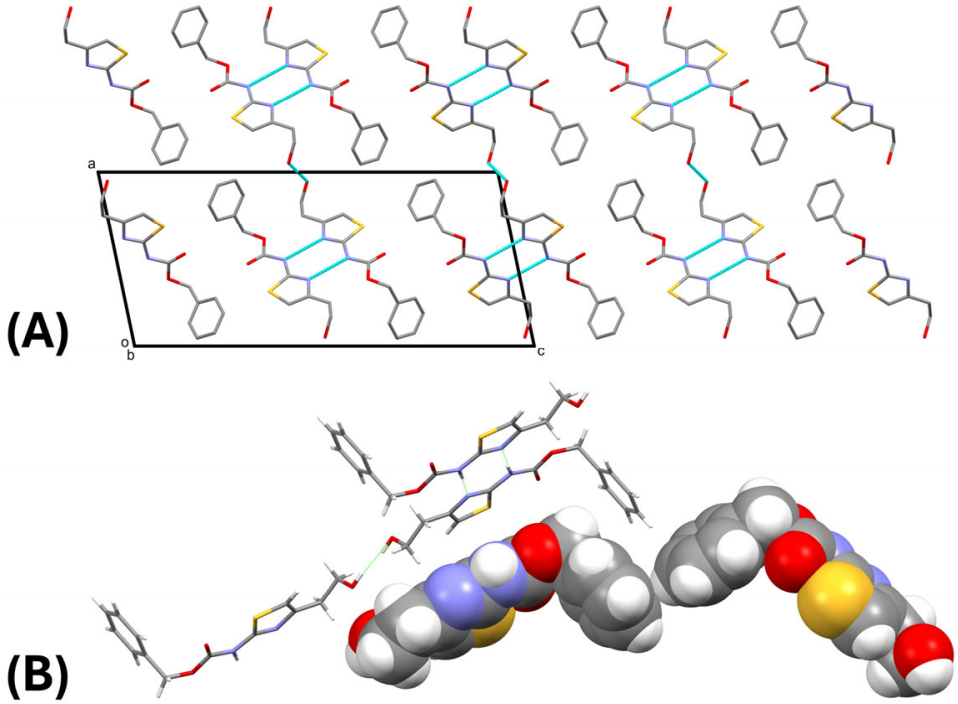

Figure 4. (**A**). Crystal packing of compound **2**, shown as a stick model along the *b* axis. Hydrogen atoms and the disorder are omitted for clarity. The main hydrogen bonds are represented as cyan lines. (**B**). Stick-spacefill model of compound **2** showing the main interactions in an arbitrary orientation. The disorder is omitted for clarity.

Table 1. Hydrogen bond geometry (D: Donor, A: Acceptor) in the crystal structure of compound **2**.

	D-H/Å	H···A/Å	D···A/Å	D-H···A/°
N2-H2···N1 ^{I}	0.92 (5)	2.09 (5)	3.012 (6)	177 (5)
O1A-H1A···O1 ^{II}	0.82 (2)	2.23 (1)	2.79 (2)	125 (1)
C13-H13···O1 ^{III}	0.93 (1)	2.76 (1)	3.52 (1)	139.8 (5)
O1-H1···O1A ^{IV}	0.82 (1)	1.92 (2)	2.73 (2)	167.9 (8)
O1-H1···O1 ^{IV}	0.82 (1)	2.29 (1)	3.02 (2)	148.7 (7)

Equivalent positions: ^{I} 1-x, 1-y, 1-z; ^{II} 2-x, -y, 1-z; ^{III} x-1, y+1, z; ^{IV} 2-x, 1-y, 1-z.

3. Materials and Methods

All reagents, chemicals, and solvents were purchased from commercial suppliers (Merck KGaA, Darmstadt, Germany; TCI Europe N.V.) and used as received. Anhydrous solvents were used as provided by the suppliers. Aluminum foil-backed silica gel 60 matrix with fluorescent indicator was used for thin-layer chromatography to follow the course of the reaction (visualization at 254 nm). A Stuart SMP 30 Mp Apparatus (Cole-Parmer Stuart, Stone, UK) was employed to measure the melting point. ^{1}H NMR and ^{13}C NMR spectra were recorded at room temperature with a Varian Oxford 300 MHz instrument (Varian, Palo Alto, CA, USA) operating at 300 MHz for ^{1}H and 75 MHz for ^{13}C.

3.1. Synthesis and Characterization of Benzyl-(4-(2-hydroxyethyl)thiazol-2-yl)carbamate

To a suspension of $LiBH_4$ (85.2 mg, 3.92 mmol) in anhydrous THF (2 mL) at −10 °C, a solution of compound **1** (200.0 mg, 0.6527 mmol) in anhydrous THF (2.5 mL) was added dropwise under a nitrogen atmosphere. The reaction mixture was allowed to gently warm up at room temperature and was stirred until TLC confirmed the disappearance of compound **1** (mobile phase cyclohexane/ethyl acetate; 7:3), which was complete after 4 h. Afterwards, water (1 mL) was slowly added, the solvent was removed, and the residue was taken up with ethyl acetate (10 mL). The organic phase was extracted with brine (2 mL), dried over Na_2SO_4, and concentrated to obtain compound **2** as a white solid (167.3 mg, 0.6012 mmol); m.p: 115.8 °C; yield: 92.5%. ^{1}H NMR (300 MHz, CD_3OD) δ 7.46–7.26 (m, 5H), 6.69 (t, *J* = 0.9 Hz, 1H), 5.24 (s, 2H), 3.80 (t, *J* = 6.7 Hz, 2H), 2.81 (td, *J* = 6.7, 0.9 Hz, 2H). ^{13}C NMR (75 MHz, CD_3OD) δ 160.02, 154.00, 148.75, 135.92, 128.17, 127.99, 127.82, 107.78, 67.21, 60.65, 34.02.

3.2. Single-Crystal X-Ray Diffraction

Benzyl-(4-(2-hydroxyethyl)thiazol-2-yl)carbamate (**2**) was crystallized by layering isopropyl ether on a solution of the compound in methanol. Colorless plates grew within one week and were harvested for single-crystal X-ray diffraction analysis. Intensity data were collected at 293 K using an Oxford Diffraction Xcalibur diffractometer (Oxford Diffraction Ltd., Abingdon, UK), equipped with a Sapphire2 CCD detector and graphite monochromator, operating at 50 kV and 40 mA with MoKα radiation. Data collection was performed using 1° φ and ω scans, with exposure times of 40 s per frame for φ scans and 60 s per frame for ω scans, up to a maximum 2θ of 23°. The crystal was determined to be metrically monoclinic, and systematic absences were compatible with space group $P2_1/c$. Lorentz-polarization and analytical absorption corrections were applied using *CrysAlisPro* (Oxford Diffraction). The structure was solved by direct methods using *SIR-2019/3* and completed by iterative cycles of full-matrix least-squares refinement on F_o^2 and Δ*F* [14] synthesis using *SHELXL-2019/3* [15] within the *WinGX* suite (*WinGX v.2023.1*) [16]. Hydrogen atoms were introduced at calculated positions in their described geometries and were allowed to ride on the attached atom with fixed isotropic thermal parameters (1.2 Ueq of the parent atom for aromatic and methylene H). The carbamate hydrogen was refined freely, with an isotropic displacement parameter. Conversely, the hydroxyl hydrogens were refined in their calculated position with fixed isotropic thermal parameters (1.5 Ueq of the parent atom) due to the disorder in the side chain. The structure was analyzed with *PARST* [17], *Mercury 2025.1.1* [18], and *Mogul* [11]; graphical representations were rendered with *Mercury*. Data collection and refinement statistics are reported in Table 2.

Table 2. Crystal data and structure refinement statistics for compound **2**.

Identification Code	**2**
Empirical formula	$C_{13}H_{14}N_2O_3S$
Formula weight	278.32
Temperature (K)	293(2)
Wavelength (Å)	0.71073
Crystal system	Monoclinic
Space group	$P2_1/c$
Unit cell dimensions (Å/°)	a = 11.0837 (11)
	b = 4.9184 (5) β = 101.858 (10)
	c = 24.941 (3)
Volume (Å^3)	1330.6 (2)
Z	4
Density calcd. (Mg/m^3)	1.389
Abs. coefficient (mm^{-1})	0.249
F(000)	584
Crystal size (mm^3)	0.12 × 0.05 × 0.01
θ range data collection (°)	2.757 to 23.257
Index ranges	$-12 \leq h \leq 12$, $-5 \leq k \leq 5$, $-27 \leq l \leq 27$
Reflections collected	20,820
Independent reflections	1910 [R_{int} = 0.0698]
Completeness to θ_{max} (%)	99.4%
Refinement method	Full-matrix least-squares on F^2
Data/restraints/parameters	1910/2/195
Goodness-of-fit on F^2	1.090
Final R indices [I > 2σ(I)]	R1 = 0.0738, wR2 = 0.1421
R indices (all data)	R1 = 0.1142, wR2 = 0.1587
Extinction coefficient	0.0040 (7)
Largest diff. peak/hole (e·Å^{-3})	0.199 and −0.214
CCDC deposition number	2467715

Supplementary Materials: Figure S1: ^{1}H NMR spectrum of compound **2** in CD_3OD; Figure S2: ^{13}C NMR spectrum of compound **2** in CD_3OD; Figure S3: TLC of the reaction (mobile phase cyclohexane/ethyl acetate; 7:3); Table S1: Atomic coordinates and equivalent isotropic displacement parameters for the crystal of compound **2**; Table S2: Bond lengths and angles for the crystal of compound **2**; Table S3: Anisotropic displacement parameters for the crystal of compound **2**. Figure S4: Photograph of the crystal of compound **2** and prediction of the crystal habit by the CLP (Coulomb–London–Pauli) model.

Author Contributions: The required synthetic step and characterization (NMR, m.p.) were carried out by L.S. The X-ray data were obtained, solved, and discussed by M.M. The study was designed by L.F. The manuscript was written by L.F. with all other authors contributing. All authors have read and agreed to the published version of the manuscript.

Funding: This research received no external funding.

Data Availability Statement: CCDC 2467715 contains the supplementary crystallographic data. These data can be obtained free of charge from the Cambridge Crystallographic Data Centre via https://www.ccdc.cam.ac.uk/structures.

Acknowledgments: M.M. sincerely thanks Diego Gatta and Nicola Rotiroti for granting access to their facilities.

Conflicts of Interest: The authors declare no conflicts of interest.

Abbreviations

The following abbreviations are used in this manuscript:

Cbz	Benzyloxycarbonyl
CCD	Charge-Coupled Device
NMR	Nuclear Magnetic Resonance
THF	Tetrahydrofuran

References

1. Prandi, C.; Occhiato, E.G. From Synthetic Control to Natural Products: A Focus on *N*-heterocycles. *Pest. Manag. Sci.* **2019**, *75*, 2385–2402. [CrossRef] [PubMed]
2. Favi, G. Modern Strategies for Heterocycle Synthesis. *Molecules* **2020**, *25*, 2476. [CrossRef] [PubMed]
3. Rizzo, C.; Pace, A.; Pibiri, I.; Buscemi, S.; Palumbo Piccionello, A. From Conventional to Sustainable Catalytic Approaches for Heterocycles Synthesis. *ChemSusChem* **2024**, *17*, e202301604. [CrossRef] [PubMed]
4. Kabir, E.; Uzzaman, M. A Review on Biological and Medicinal Impact of Heterocyclic Compounds. *Results Chem.* **2022**, *4*, 100606. [CrossRef]
5. Rusu, A.; Moga, I.-M.; Uncu, L.; Hancu, G. The Role of Five-Membered Heterocycles in the Molecular Structure of Antibacterial Drugs Used in Therapy. *Pharmaceutics* **2023**, *15*, 2554. [CrossRef] [PubMed]
6. Arshad, M.F.; Alam, A.; Alshammari, A.A.; Alhazza, M.B.; Alzimam, I.M.; Alam, M.A.; Mustafa, G.; Ansari, M.S.; Alotaibi, A.M.; Alotaibi, A.A.; et al. Thiazole: A Versatile Standalone Moiety Contributing to the Development of Various Drugs and Biologically Active Agents. *Molecules* **2022**, *27*, 3994. [CrossRef] [PubMed]
7. Liebeschuetz, J.W.; Murray, C.W.; Young, S.C.; Camp, N.P.; Jones, S.D.; Wylie, W.A.; Master, J.J. Serine Protease Inhibitors 2001. Eli Lilly and Company. WO 01/96323 A1.
8. Břehová, P.; Chaloupecká, E.; Česnek, M.; Skácel, J.; Dračínský, M.; Tloušťová, E.; Mertlíková-Kaiserová, H.; Soto-Velasquez, M.P.; Watts, V.J.; Janeba, Z. Acyclic Nucleoside Phosphonates with 2-Aminothiazole Base as Inhibitors of Bacterial and Mammalian Adenylate Cyclases. *Eur. J. Med. Chem.* **2021**, *222*, 113581. [CrossRef] [PubMed]
9. Decuyper, L.; Jukič, M.; Sosič, I.; Žula, A.; D'hooghe, M.; Gobec, S. Antibacterial and B-Lactamase Inhibitory Activity of Monocyclic B-Lactams. *Med. Res. Rev.* **2018**, *38*, 426–503. [CrossRef] [PubMed]
10. Inoue, T.; Morita, M.; Tojo, T.; Yoshihara, K.; Nagashima, A.; Moritomo, A.; Ohkubo, M.; Miyake, H. Synthesis and SAR Study of New Thiazole Derivatives as Vascular Adhesion Protein-1 (VAP-1) Inhibitors for the Treatment of Diabetic Macular Edema. *Bioorg. Med. Chem.* **2013**, *21*, 1219–1233. [CrossRef] [PubMed]
11. Bruno, I.J.; Cole, J.C.; Kessler, M.; Luo, J.; Motherwell, W.D.S.; Purkis, L.H.; Smith, B.R.; Taylor, R.; Cooper, R.I.; Harris, S.E.; et al. Retrieval of Crystallographically-Derived Molecular Geometry Information. *J. Chem. Inf. Comput. Sci.* **2004**, *44*, 2133–2144. [CrossRef] [PubMed]
12. Haroon, M.; Akhtar, T.; Yousuf, M.; Baig, M.W.; Tahir, M.N.; Rasheed, L. Synthesis, Spectroscopic Characterization and Crystallographic Behavior of Ethyl 2-(4-Methyl-(2-Benzylidenehydrazinyl))Thiazole-4-Carboxylate: Experimental and Theoretical (DFT) Studies. *J. Mol. Struct.* **2018**, *1167*, 154–160. [CrossRef]
13. Cazzaniga, G.; Mori, M.; Meneghetti, F.; Chiarelli, L.R.; Stelitano, G.; Caligiuri, I.; Rizzolio, F.; Ciceri, S.; Poli, G.; Staver, D.; et al. Virtual Screening and Crystallographic Studies Reveal an Unexpected γ-Lactone Derivative Active against MptpB as a Potential Antitubercular Agent. *Eur. J. Med. Chem.* **2022**, *234*, 114235. [CrossRef] [PubMed]
14. Burla, M.C.; Caliandro, R.; Carrozzini, B.; Cascarano, G.L.; Cuocci, C.; Giacovazzo, C.; Mallamo, M.; Mazzone, A.; Polidori, G. Crystal Structure Determination and Refinement *via SIR2014*. *J. Appl. Crystallogr.* **2015**, *48*, 306–309. [CrossRef]
15. Sheldrick, G.M. Crystal Structure Refinement with *SHELXL*. *Acta Crystallogr. C Struct. Chem.* **2015**, *71*, 3–8. [CrossRef] [PubMed]
16. Farrugia, L.J. *WinGX* and *ORTEP for Windows*: An Update. *J. Appl. Crystallogr.* **2012**, *45*, 849–854. [CrossRef]
17. Nardelli, M. *PARST* 95—An Update to *PARST*: A System of Fortran Routines for Calculating Molecular Structure Parameters from the Results of Crystal Structure Analyses. *J. Appl. Crystallogr.* **1995**, *28*, 659. [CrossRef]
18. Macrae, C.F.; Sovago, I.; Cottrell, S.J.; Galek, P.T.A.; McCabe, P.; Pidcock, E.; Platings, M.; Shields, G.P.; Stevens, J.S.; Towler, M.; et al. *Mercury 4.0*: From Visualization to Analysis, Design and Prediction. *J. Appl. Crystallogr.* **2020**, *53*, 226–235. [CrossRef] [PubMed]